physics

MDPI

Article

Cosmological Constraints on the Formation and Survival of Small Hydrogen

Jerry Va'vra

SLAC (Stanford Linear Accelerator Center), Menlo Park, CA 94025-701, USA; jjv@slac.stanford.edu

Abstract

The paper investigates the possibility of small hydrogen (SH) formation in the early Universe during an interval of about 10–80 s after the Big Bang. Assuming that SH exists as proposed by the author earlier, the current study examines the cosmological conditions under which the SH can be formed and survive. The photon, baryon, and electron–positron pair densities are estimated, together with the corresponding thermal energies and temperatures, and the formation cross section required to obtain a specified SH abundance and the maximum destruction cross section consistent with SH survival are derived. Although the microscopic formation and destruction cross sections are not presently known, phenomenological constraints the cross sections must satisfy are derived for a given SH abundance. The study suggests that, if SH exists and has negligible nuclear interactions, it would not significantly participate in the standard Big Bang nucleosynthesis reaction network. The possibility that SH can undergo early cosmological decoupling, subject to the presently unknown momentum-transfer cross sections, is also discussed. If SH is formed in sufficient abundance and decouples sufficiently early, it can provide an interesting mechanism for early structure formation and may potentially contribute to the formation of black-hole seeds. This study does not establish the existence of SH, but rather examines whether the conditions in the early Universe present immediate cosmological obstacles to SH formation and survival.

Keywords: small hydrogen; relativistic bound states; virial theorem; femtometer-scale atoms; early Universe; cosmological decoupling

Received: 20 June 2026
Revised: 31 July 2026
Accepted: 12 August 2026
Published: 8 September 2026

1. Introduction

Earlier, the author has investigated [1] whether a formation of a compact electron–proton configuration ("small hydrogen", SH) with a characteristic radius of a few femtometers is compatible with relativistic kinematics and simple stationarity constraints. The SH model employs the following three principal assumptions:

- the relativistic virial-stability condition,
- the relativistic de Broglie standing-wave condition, $2\pi r = n \cdot \lambda_{\text{de Broglie}}$, where r is the electron orbital radius, n is an integer and $\lambda_{\text{de Broglie}}$ is the de Broglie wavelength, and
- the requirement of negative total binding energy.

Together, these conditions determine the characteristic SH radius and binding energy within the phenomenological model developed in Ref. [1]. The framework is not intended to establish the existence, formation probability, lifetime, or dynamical stability of SH. Rather, it is examined whether relativistic kinematics, finite-size effects, and virial-inspired stationarity constraints by themselves preclude such compact configurations. The model is phenomenological and does not rely on Dirac or QED (quantum electrodynamics) bound-state eigenvalues. The resulting characteristic energy scales—a central binding energy scale of approximately 260 keV and a spin splitting of approximately 100 ± 20 keV—define concrete experimental and observational energy ranges of interest.

The present paper adopts the SH parameters inferred in Ref. [1] as working assumptions and investigates whether the conditions in the early Universe are compatible with SH formation and survival. The objective is not to rederive the SH model, but to investigate the cosmological consequences if the phenomenological parameters obtained in Ref. [1] are realized in nature.

Table 1 shows basic parameters of SH and compares them to normal hydrogen. The important feature of SH, apart from its size, is its binding energy E_b. Depending on electron spin orientation, it is either −204 keV or −308 keV. The energy range in which SH survival against photodissociation is expected to improve is $kT \leq 300$ keV (where k is the Bolzmann constant and T is the absolute temperature), corresponding to the SH binding energy scale. The SH mass in Table 1 is calculated as follows: $M_{SH} = m_p + \gamma_e\, m_e - |U|/c^2$, where m_p *is* the proton mass, m_e is the electron mass, γ_e is the electron Lorentz factor, c is the speed of light, and U is the total interaction energy.

Table 1. Small hydrogen and normal hydrogen properties.

Quantity	Normal Hydrogen	Small Hydrogen
Electron radius r_e	0.529 Å	2.845 fm
Electron de Broglie wavelength λ_e	3.322 Å	17.88 fm
Electron de Broglie wave frequency f_e	~6.6 × 10^{15} Hz	~1.68 × 10^{22} Hz
Electron $\beta_e = v/c$ (v is electron velocity and c the speed of light)	~7.3 × 10^{-3}	~0.9999729
Electron Lorentz factor γ_e	1.0000266	135.746
Composite mass M_{SH}	1.78 MeV/c^2	938.63 MeV/c^2
Binding energy E_b	−13.6 eV	−204 keV (spin +) −308 keV (spin −)

Although SH differs from dark-atom models proposed in the dark matter literature, both objects involve compact neutral bound states and raise related questions concerning formation, survival, and cosmological evolution [2–4].

2. Early Universe Density of Photons, Baryons and e^+e^- Pairs

In Ref. [1], it is suggested that SH can be produced in the collapse of very massive stars, where electron densities can reach values approaching 10^{37} cm^{-3}. Under such conditions, the plasma frequency may approach 10^{22} Hz, comparable to the characteristic de Broglie frequency associated with SH. This observation motivated the hypothesis that collective plasma processes may contribute to SH formation. However, the detailed microscopic formation mechanism remains unknown.

The present study investigates a different environment: the early Universe shortly before and during Big Bang nucleosynthesis (BBN) [5]. Rather than assuming a specific formation mechanism, the question is raised whether the early Universe plasma provides conditions compatible with SH formation and survival of the latter. This is a period when the Universe was hot, with the standard cosmological model predicting thermal energies kT between about 50 and 500 keV, corresponding to temperatures between about 6 × 10^8 and 6 × 10^9 K. During this period, the early Universe is considered to have exceptionally large densities of photons and e^+e^- pairs. As shown in Figure 1, the Universe is dominated by photons and e^+e^- pairs, while the baryon density is substantially lower. Figure 1 also shows that the e^+e^- pair density decreases below a thermal energy of approximately 50 keV. The corresponding expressions are summarized in Appendix A.

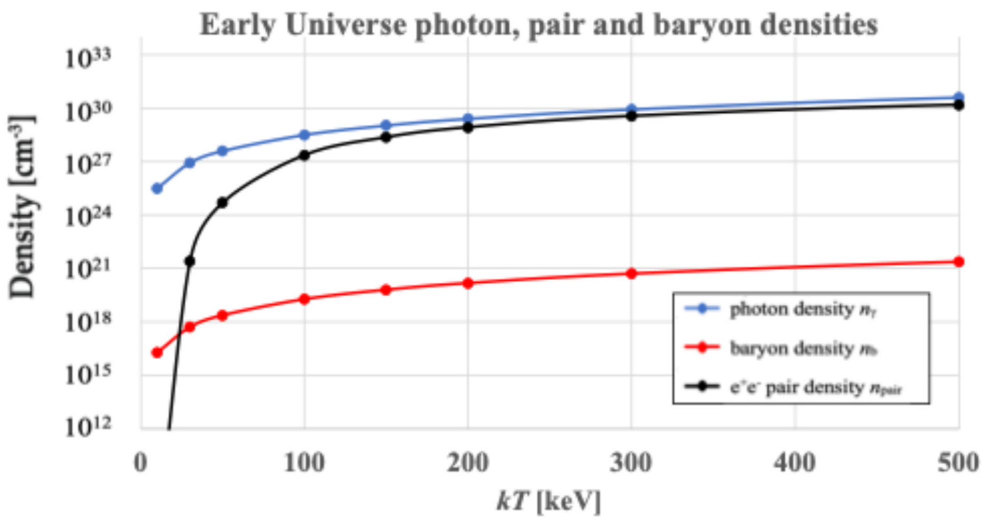

Figure 1. Early Universe photon, e^+e^- pair, and baryon densities as a function of thermal energy kT. See text for details.

Figure 2 shows a cosmological time profile of the density development (see Appendix B). One can find that the time interval corresponding to the thermal energy window of 50–300 keV is estimated as about 8–300 s after the Big Bang. This interval defines a natural candidate window for SH formation, within the assumptions of the present phenomenological model.

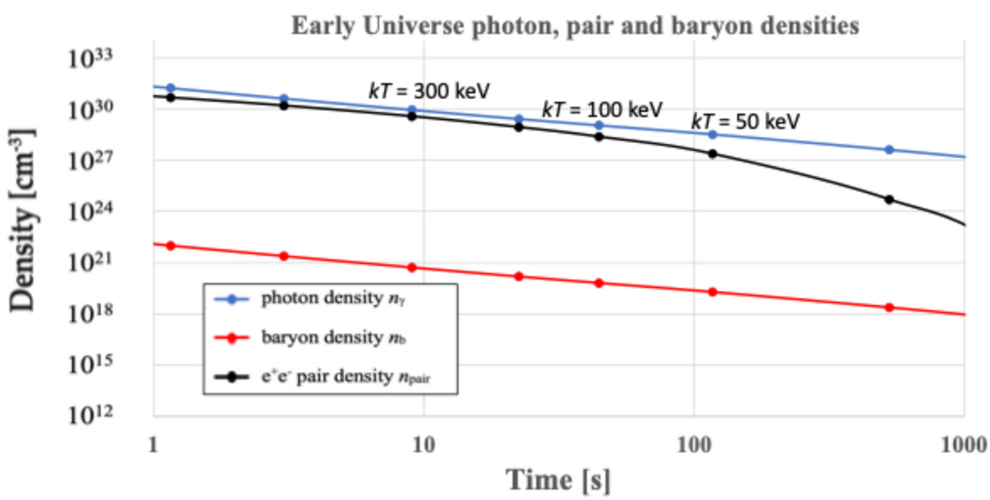

Figure 2. Time evolution of photon, baryon, and e^+e^- pair densities in the radiation-dominated Universe. The cosmological time is calculated using equations in Appendix B, including the temperature-dependent effective number of relativistic degrees of freedom $g_*(T)$.

Figures 1 and 2 show that the early Universe contains pair-electron densities approaching 10^{28}–10^{32} cm^{-3}. Although these densities are several orders of magnitude lower than those expected in the collapse of the most massive stars, they remain extraordinarily large by laboratory standards. Based on the electron density listed in Table 2, the corresponding plasma frequencies reach values up to about 10^{19} Hz in the thermal energy range 100–300 keV. Whether such conditions are sufficient for SH formation remains unknown;

however, the enormous pair-electron abundance motivates investigating the required formation cross sections in this environment.

Table 2. Summary of "interesting epochs" relevant to this paper ($n_{pair} = n_{e-} + n_{e+}$). See text for details.

kT [keV]	Time [s]	$n_e = n_{pair}/2$ [cm^{-3}]	n_γ [cm^{-3}]	n_b [cm^{-3}]
300	8.2	~1.9×10^{29}	~8.5×10^{29}	~5.1×10^{20}
100	74	~1.15×10^{27}	~3.2×10^{28}	~1.9×10^{19}
50	296	~2.45×10^{24}	~5.3×10^{27}	~2.4×10^{18}

Table 2 illustrates that throughout the 50–300 keV interval the free-electron density n_e exceeds the baryon density by many orders of magnitude, while the photon density remains the dominant component of the plasma.

The quantities shown in Figures 1 and 2 vary rapidly during the epoch of interest. Therefore, the formation and destruction probabilities derived in the following sections are expressed as time integrals over the cosmological evolution, rather than evaluated at a single temperature.

3. Formation of Small Hydrogen

Figure 3 shows that the ratio of the number of e^+e^- pairs to the number of baryons is $n_{pair}/n_b > 10^8$ and holds during about the first 100 s after the Big Bang, after which it decreases significantly. The pair-electron density exceeds the baryon density by more than eight orders of magnitude throughout this period. Consequently, the availability of electrons is not expected to be the limiting factor for SH formation.

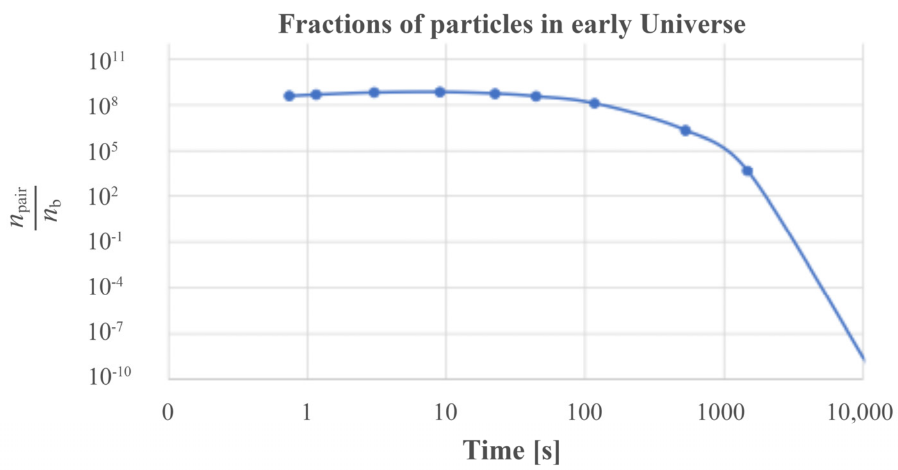

Figure 3. Ratio of the number of electron–positron pairs to the number of baryons as a function of cosmological time $t(kT)$ during the radiation-dominated era.

The formation process may be represented schematically as $p + e^- + X \rightarrow SH + X'$, where X denotes the surrounding plasma, collective plasma excitations, or another particle capable of carrying away energy and momentum. The auxiliary system X is required to carry away the binding energy and momentum. The key problem is that forming SH requires disposing of the binding energy $E_b \approx$ 200–300 keV. For normal hydrogen, the energy corresponding to the binding energy is carried away by a photon. In the SH case, the energy might be carried away by plasma oscillations, scattering from another e^+ or e^-, emission of a photon, or collective electric-field fluctuations. The absolute value of the SH formation cross section is not known in such an e^+e^- plasma environment at kT = 50–300 keV.

However, one can question what can be a required cross section $\sigma_{\mathrm{form}}^{\mathrm{req}}$ to achieve a certain SH abundance among baryons. More generally, the formation probability is

$$P_{\mathrm{form}} = \int_{t_i}^{t_f} n_e(t)\, \sigma_{\mathrm{form}} v_{\mathrm{rel}}\, dt,$$

where t_i and t_f denote the initial and final times, respectively, of the epoch over which SH formation is assumed to occur, corresponding approximately to the thermal energy interval kT = 300–50 keV in the present study. Here, n_e(t) is the free-electron density and v_{rel} is the relative proton–electron velocity. If the formation cross section varies only quite weakly over the temperature interval of interest and $v_{\mathrm{rel}} \approx c$, the formation probability becomes $P_{\mathrm{form}} \propto n_e(kT)\, \sigma_{\mathrm{form}}\, c\, t(kT)$.

Under this approximation, the required formation cross section becomes

$$\sigma_{\mathrm{form}}^{\mathrm{req}} = \frac{f_{\mathrm{SH}}}{n_e(kT)\, c\, t(kT)}, \tag{1}$$

where f_{SH} is the desired abundance fraction of SH, $n_e(kT) = n_{\mathrm{pair}}(kT)/2$ is the free-electron density (Appendix A), c is the speed of light, and $t(kT)$ is cosmological time (see Appendix B). The parameter f_{SH} denotes the assumed SH abundance, which is defined as

$$f_{\mathrm{SH}} = \frac{\text{number of baryons hidden in SH}}{\text{number of free baryons in standard cosmology}}. \tag{2}$$

Figure 4 shows the required cross section $\sigma_{\mathrm{form}}^{\mathrm{req}}$ for the formation of SH in the Early Universe for several choices of the abundance factor f_{SH}. At low thermal energies such as below about 50 keV, the e^+e^- pair density drops rapidly enough, and therefore a larger formation cross section is needed. At high thermal energies, the two effects largely compensate each other, producing the broad plateau seen in Figure 4. The $\sigma_{\mathrm{form}}^{\mathrm{req}}$ cross section values are considerably small in the thermal energy interval of 100–300 keV. For example, for f_{SH} = 0.01 (1% of baryon matter ends up in the form of SH), cross section values are between 10^{-43} and 10^{-42} cm^2. These values are exraordinary small compared with typical atomic and nuclear cross sections.

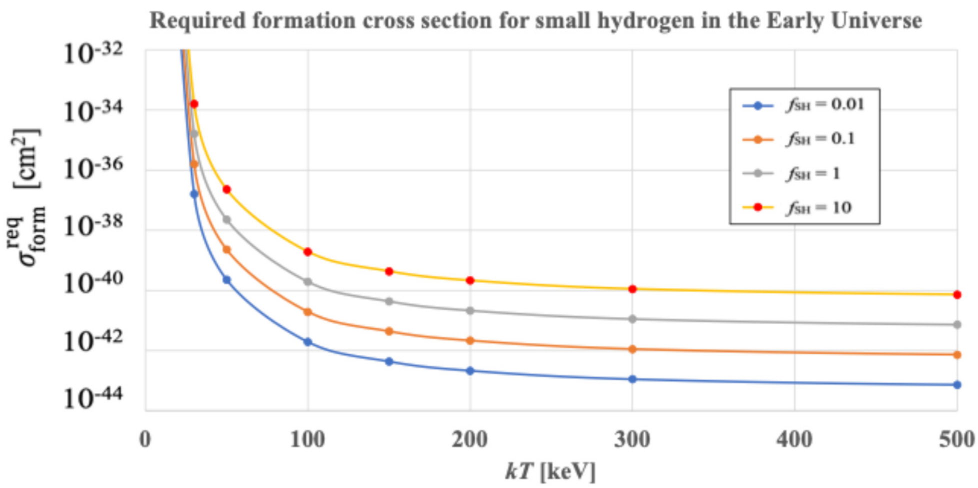

Figure 4. Required SH formation cross section in the early Universe for several assumed abundance fractions f_{SH}.

The present study does not identify a specific microscopic mechanism capable of producing SH with cross sections in the range 10^{-43}–10^{-41} cm^2. The required coupling between protons, electrons, and collective plasma excitations in a dense e^+e^- environment remains unknown. The purpose of the present calculation is therefore not to predict the formation cross section, but rather to determine the range of cross sections required to obtain a specified SH abundance.

4. Does Formation of Small Hydrogen Affect Friedmann Expansion?

Given the assumptions adopted in this study, their self-consistency should be verified. If a fraction f_{SH} of the baryons becomes bound into SH during the radiation-dominated era, it is helpful to verify that the corresponding SH rest-mass energy density remains much smaller than the radiation energy density. To address this question, let us compare the rest-mass energy density associated with baryons bound in SH $\rho_{SH} = f_{SH}\, n_b\, M_{SH}\, c^2$, with radiation density $\rho_{rad} = \langle E_\gamma \rangle\, n_\gamma = 2.7\, kT\, n_\gamma$, where the angular brackets denote the average photon energy over the thermal Planck distribution (see Appendix A for calculation of n_b and n_γ). Figure 5 shows that $\rho_{SH} \ll \rho_{rad}$ even for very large SH abundance factor f_{SH} in the thermal energies range between 100 and 300 keV. Therefore, the Universe remains radiation-dominated even for such a large SH abundance and follows the Friedmann equation $H^2 = (8\pi G/3)\rho_{rad}$ (with H the Hubble parameter and G the Newton's gravitational constant), which implies that the radiation-dominated relation $t(kT)$ used throughout this paper remains self-consistent. The standard radiation-dominated expansion is therefore expected to remain essentially unchanged over the temperature interval considered here. Figure 5 shows that radiation energy density dominates strongly during this epoch, implying that even substantial SH abundances do not significantly alter the Friedmann expansion rate. This comparison should be regarded as a consistency check of the assumptions used in the present study rather than as evidence for the existence of SH.

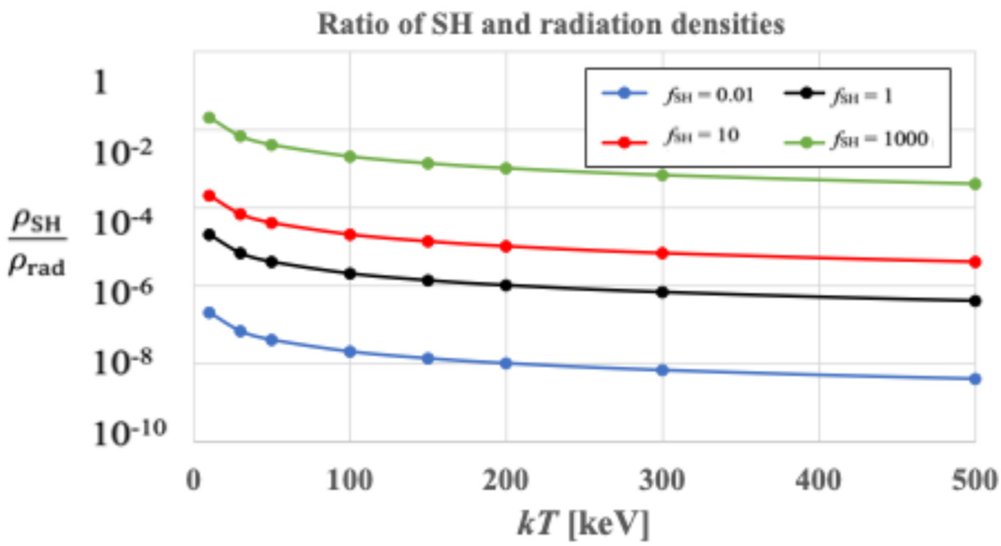

Figure 5. Ratio of SH rest-mass energy density to radiation energy density as a function of thermal energy for the four assumed SH abundance factors f_{SH}, as indicated.

The conclusion that SH does not significantly affect the expansion history is not, by itself, sufficient to establish consistency with BBN. In addition, SH must remain largely inert with respect to the standard nucleosynthesis reactions. In the present exploratory study, let us therefore consider the limiting case in which SH neither participates significantly in nuclear reactions nor catalyzes light-element production. Under this assumption, the dominant effect of SH is gravitational, while standard BBN proceeds using the baryons that remain available for nucleosynthesis.

Because $\rho_{rad} \propto T^4$ whereas the SH rest-mass density scales approximately as T^3, the ratio $\rho_{SH}/\rho_{rad} \propto 1/kT$. Consequently, the relative SH contribution grows as the Universe cools, but this contribution remains subdominant throughout the temperature interval considered here.

5. Small Hydrogen Photon Dissociation

Assuming that SH is created in the hot e^+e^- plasma during the first few hundred seconds after the Big Bang, it is also subject to destruction through photodissociation $\gamma + \mathrm{SH} \to p + e^-$. The actual SH photodissociation cross section $\sigma_{\gamma\mathrm{SH}}$ is presently unknown. The number of photons capable of dissociating SH is not the total photon density $n_\gamma^{\mathrm{total}}$, but only the fraction with energies exceeding the binding energy $|E_\mathrm{b}|$. This fraction is shown in Figure 6 and is discussed in Appendix E. It decreases rapidly as kT falls below $|E_\mathrm{b}|$, thereby suppressing photodissociation.

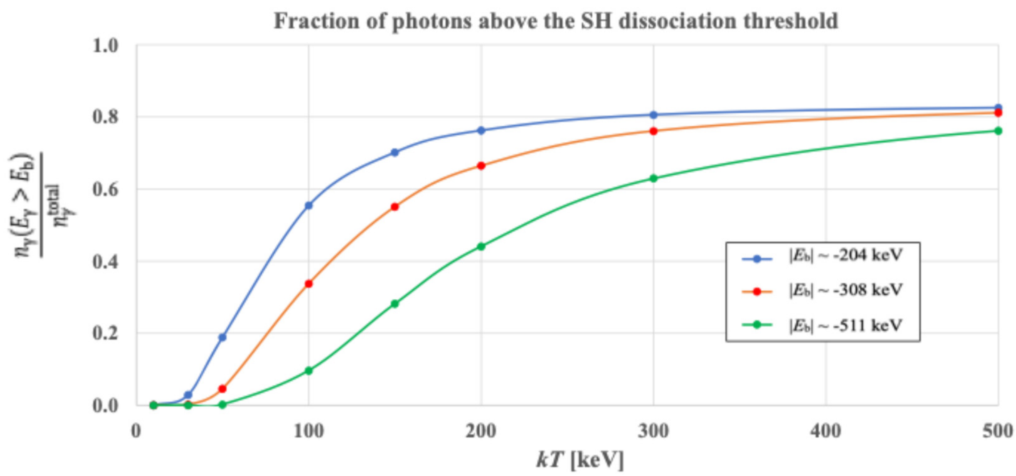

Figure 6. Fraction of photons in a Planck distribution with energies exceeding the SH dissociation threshold for three values of assumed SH binding energies as indicated. The curves are based on the approximation of Equation (A2), which becomes increasingly accurate for $|E_\mathrm{b}|/kT \geq 2$. The approximation becomes less accurate near $kT \approx 500$ keV, and the corresponding values should therefore be regarded as approximate.

Rather than attempting to calculate $\sigma_{\gamma\mathrm{SH}}$, let us determine the largest photodissociation cross section $\sigma_{\mathrm{dest}}^{\mathrm{max}}$ compatible with SH survival. The derivation is given in Appendix E and gives

$$\sigma_{\mathrm{dest}}^{\mathrm{max}} = \frac{1}{n_\gamma(E_\gamma > |E_\mathrm{b}|)c\, t(kT)}. \tag{3}$$

Using the approximation given in Appendix E, Figure 7 shows that the fraction of photons capable of dissociating SH decreases rapidly as the temperature falls below the binding energy scale. The two curves merge above 300 keV. This indicates that the precise value of the binding energy becomes less significant at relatively high temperatures. However, below 100–150 keV, the state with larger binding energy is less susceptible to photodissociation. Curves approaching about 500 keV are approximate.

The formation and cross section processes may be combined into a single constrained diagram. For each temperature, one may determine both the required cross section $\sigma_{\mathrm{form}}^{\mathrm{req}}$ and the maximum allowed destruction cross-section $\sigma_{\mathrm{dest}}^{\mathrm{max}}$. Figure 8 therefore defines the region of parameter space in which SH formation and survival are simultaneously possible. Figure 8 identifies the region of parameter space in which SH can both form and survive in the early Universe.

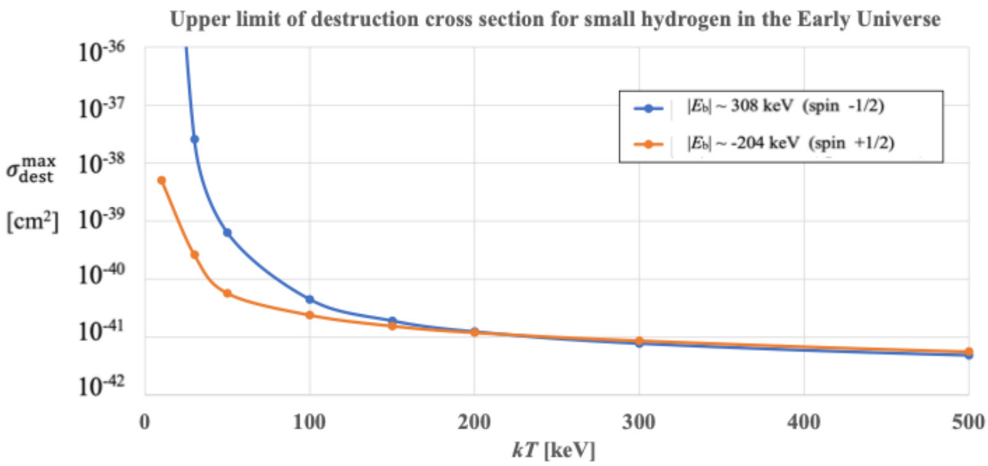

Figure 7. Maximum destruction cross section for SH photon dissociation as a function of thermal energy for two values of SH binding energies.

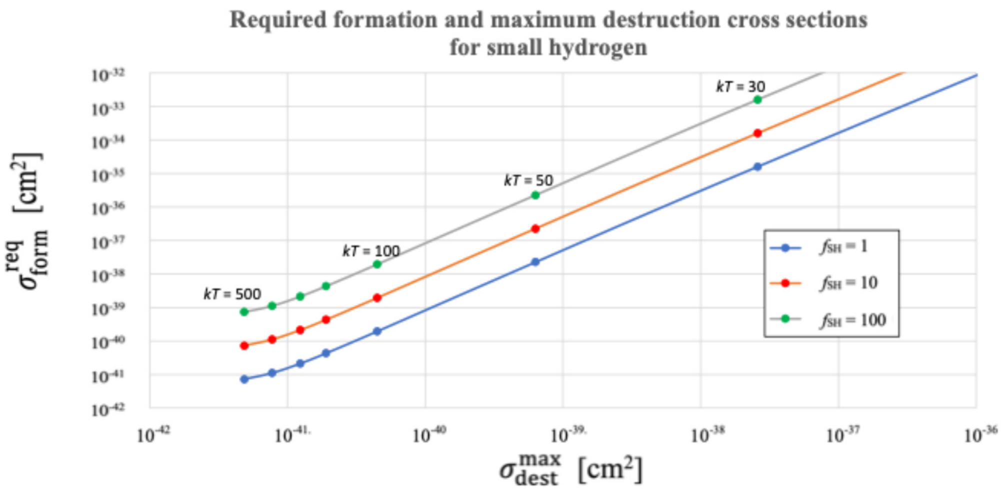

Figure 8. Required formation cross section for each value of maximum cross section for the three SH values of f_{SH} parameter, as indicated. Calculations assume the spin $-1/2$ state with binding energy $|E_b|$ = 308 keV. Thermal energy kT values are given in keV units.

6. Conclusions

The early Universe environment does not by itself rule out the formation of SH, although SH viability depends on two presently unknown microscopic quantities: the formation cross section and the photodissociation (destruction) cross section. The present study converts this cosmological question into quantitative requirements on those cross sections.

It is shown that the early Universe environment does not exclude SH formation during the 100–300 keV epoch, provided the formation cross section is at least as large as the required values estimated here. During this period, the e^+e^- pair density is exceptionally high compared with the baryon density, and the required formation cross sections needed to achieve a specified SH abundance are correspondingly extraordinarily small. The maximum photodissociation cross section compatible with SH survival is also estimated.

The study performed indicates that SH formation and survival are simultaneously possible during the interval in which the thermal energy lies between approximately 100 and 300 keV, corresponding to cosmological times between about 10 and 500 s after the Big Bang. It is further found that the SH energy density remains much smaller than the radiation energy density throughout this epoch. Consequently, even substantial SH abundances do not significantly modify the radiation-dominated Friedmann expansion, and the cosmological framework used throughout the study remains self-consistent.

Qualitative arguments suggesting that SH may interact only weakly with the standard BBN reaction network are also presented, although the relevant nuclear interaction cross sections remain unknown and require further investigation before firm conclusions can be drawn.

Finally, if SH forms in significant abundance and survives photodissociation, it may decouple from the primordial plasma on a timescale of the level of 8–500 s, dramatically earlier than ordinary hydrogen, which decouples approximately 380,000 years after the Big Bang. If SH remains effectively decoupled from the radiation background, it may provide an additional matter component capable of gravitational clustering at much earlier times than ordinary hydrogen. In that respect, SH will behave in several respects similarly to a dark matter component rather than ordinary baryonic matter, which remains coupled to radiation until recombination. Whether such a component can significantly enhance early structure formation or contribute to black-hole seed formation requires a dedicated study of the growth of SH density perturbations which lies beyond the scope of the present paper [6–8].

The present study does not establish the existence of SH. Rather, it identifies a cosmological window in which its formation and survival are not excluded and formulates quantitative requirements on the corresponding formation and destruction cross sections. If SH exists and decouples from the primordial plasma at such early times, it is natural to question whether it will influence the subsequent growth of cosmic structure. This question provides an important motivation for the present study. Appendix F summarizes the principal open problems and outlines future theoretical, experimental, and cosmological investigations to assess the viability of the SH hypothesis.

Beyond cosmological considerations, Ref. [1] identified potential observational signatures of SH, including predicted characteristic gamma-ray lines and anomalous electron–proton resonances. Searches for such signatures in existing astrophysical and accelerator data is believed to provide an independent test of the SH hypothesis.

Funding: This research received no external funding.

Data Availability Statement: No new data were created or analyzed in this study. Data sharing is not applicable to this article.

Acknowledgments: I thank Robert Wagoner for discussing some details of the BBN model.

Conflicts of Interest: The author declares no conflicts of interest.

Appendix A. Early Universe Densities

Total Photon Density in Early Universe

In the context of Bose–Einstein statistics, the Riemann zeta function $\zeta(3)$ is a critical mathematical constant used to determine the thermodynamic properties of a three-dimensional, non-interacting (ideal) gas of bosons, particularly relating to photons (black-body radiation) [9–11].

For a gas of photons (massless bosons) in a three-dimensional volume, the total number of photons, n_γ, is as follows: $n_\gamma = (2\,\zeta(3)/\pi^2)(kT/\hbar c)^3 \approx 3.17 \times 10^{31} \times (kT/1\ \text{MeV})^3\ \text{cm}^{-3}$, where $\zeta(3) = \sum_{n=1}^{\infty} 1/n^3 = 1.2020569$ is the Riemann zeta function and $\hbar$ is the reduced Planck constant. One can find that for thermal energy kT of about 10 keV, the total photon density is $n_\gamma \approx 3.2 \times 10^{25}$ photons/cm^3 in early Universe.

Total Baryon Density in Early Universe

In the first fractions of a second after the Big Bang, matter and antimatter are considered to be created and annihilated in nearly equal amounts. If the symmetry had been perfect, all particles would have annihilated into pure radiation. However, a tiny, so far unexplained imbalance (known as baryogenesis) left behind roughly one extra baryon for every billion pairs that were destroyed. This asymmetry is the origin of the $\eta \approx (6 \pm 0.1) \times 10^{-10}$ ratio, setting the amount of matter in the universe. Observations of the CMB (cosmic microwave background) and elemental abundances are consistent with this ratio [5,12,13]. The resulting total baryon density is $n_b = \eta\, n_\gamma \approx 6 \times 10^{-10}\, n_\gamma$, ranging from 1.9×10^{16} to 4×10^{21} cm^{-3} for thermal energy range between 10 and 500 keV.

Total Density of e^+e^- Pairs in the Early Universe

The equilibrium density of electrons and positrons is described by the relativistic Fermi–Dirac distribution $n_{e\mp} = \frac{2}{2\pi^2\hbar^3}\int_0^\infty \frac{p^2 dp}{e^{(E/kT)}+1}$, where $E = \sqrt{p^2c^2 + m_e{}^2c^4}$. Total pair density is $n_{pair} = n_{e-} + n_{e+}$. In the non-relativistic limit ($kT \ll m_e c^2$), this reduces to the familiar Maxwell–Boltzmann approximation $n_{pair} \propto 4\left(m_e kT/2\pi\hbar^2\right)^{3/2}\exp\left(-m_e c^2/kT\right)$.

Throughout the temperature interval of 50–300 keV considered in this paper, unless stated otherwise, the numerical calculations presented employ the relativistic Fermi–Dirac expression, while the Maxwell–Boltzmann formula is included because it provides a helpful analytical approximation at lower temperatures.

Appendix B. Cosmological Time in Radiation-Dominated Early Universe

The cosmological time is obtained from the Friedmann equation for a radiation-dominated Universe, $H^2 = \left(\frac{da/dt}{a}\right)^2 = \frac{8\pi G}{3}\rho$, where H is the Hubble parameter, a is the cosmological scale factor, G is Newton's gravitational constant, and ρ is the total energy density.

During the epoch considered here ($kT \approx$ 50–500 keV), the Universe is considered radiation-dominated. The radiation energy density is $\rho_{rad} = \frac{\pi^2}{30} g_*(T)\frac{(kT)^4}{(\hbar c)^3 c^2}$, where $g_*(T)$ is the effective number of relativistic degrees of freedom. Around the epoch of electron–positron annihilation, $g_*(T)$ changes only moderately, from approximately 10.75 above annihilation to about 3.36 after annihilation.

Combining the Friedmann equation with the radiation energy density gives the standard relation $t(T) \cong 0.74\left(\frac{10.75}{g_*(T)}\right)^{1/2}\left(\frac{1\text{ MeV}}{kT}\right)^2$ s. The cosmological times used throughout this paper are calculated using this expression. Over the temperature interval of 50–300 keV considered here, the variation of $g_*(T)$ introduces only a modest correction to the familiar $t \propto T^{-2}$ scaling. The values of $g_*(T)$ are taken from the standard cosmological model [7].

Appendix C. Early Universe Cosmological Decoupling

Neutrino Decoupling

At temperatures of $kT \approx 1$ MeV, neutrinos decouple from the primordial plasma and subsequently free-stream through the expanding Universe. Their decoupling provides a helpful cosmological reference point for comparing the possible decoupling of SH.

Expected SH Decoupling

SH is electrically neutral and highly compact ($r \approx 2.84$ fm). At kT = 200–300 keV, the thermal de Broglie wavelengths are

- for electrons: $\lambda_e \approx 2000$ fm,
- for protons: $\lambda_p \approx 50$ fm,
- for photons: $\lambda_\gamma \approx$ 4000–6000 fm.

Since these probe wavelengths highly exceed the SH radius, the surrounding plasma is expected to have only limited ability to resolve the internal structure of SH. Consequently, because SH is electrically neutral and may possess only a considerably small permanent electric dipole moment, its interaction cross sections with photons and charged particles may be strongly suppressed. A quantitative determination of these cross sections remains an open problem and lies outside the scope of the present study. As the Universe cools below the SH binding energy scale ($|E_b| \approx$ 200–300 keV, depending on spin orientation), photodissociation becomes exponentially suppressed. Consequently, SH is expected to decouple from the surrounding radiation field once the temperature falls sufficiently below its binding energy. The corresponding photodissociation constraints are discussed in Appendix D.

Robert Wagoner pointed out that any new bound state participating in BBN must not significantly alter the successful predictions of standard nucleosynthesis.

The electron in SH occupies a highly relativistic compact orbit with characteristic momentum of about 70 MeV/c corresponding to $\gamma_e \approx 137$ [1]. Incorporating such a compact relativistic electron into a nuclear state requires a substantial rearrangement of the internal SH structure along with the transfer of hundreds of keV of binding energy. The compact size and highly relativistic internal electron motion suggest that SH capture by light nuclei may be strongly suppressed. A quantitative assessment requires calculation of the SH-nucleus interaction cross sections, which are presently unknown. However, one must admit that the cross sections for SH nuclear interactions remain unknown. If SH is not part of BBN, then BBN does not count hidden baryons in SH; BBN only processes the baryons that remain available for deuterium and helium formation. Under this assumption, the standard BBN predictions remains essentially unchanged because only the baryons not bound in SH participate in nucleosynthesis. However, BBN and the CMB agree on the baryon density, and therefore this point argues that $f_{SH} \ll 1$. If f_{SH} approaches unity or exceeds it, one would likely need to revisit both BBN and CMB constraints [13,14]. However, the remarkable possibility is as follows: the hidden component may not behave like ordinary baryons. If SH is neutral, decouples early enough, does not participate in nuclear reactions, and clusters gravitationally, then the CMB does not infer SH formation in exactly the same way it infers formation of ordinary baryons. Under these assumptions, SH shares several phenomenological properties commonly associated with dark matter, while remaining baryonic in origin.

For comparison, ordinary hydrogen recombines approximately 380,000 years after the Big Bang.

On the other hand, SH may decouple from radiation/plasma much earlier (approximately 10–500 s after the Big Bang) than normal hydrogen or other hadrons, shortly after neutrino decoupling. This possibility motivates the present investigation of SH formation and survival in the early Universe.

Appendix D. Possible Photodissociation Cross Section

Figure A1 presents illustrative estimates of the SH photodissociation cross sections $\sigma_{\gamma SH} \propto \sigma_0\,(kr)^m$, assuming multipole suppression, where the radius r = 2.84 fm for SH [1], binding energy $E_b = -308$ keV, photon wavelength $\lambda_\gamma = \hbar c/E_\gamma \approx 657$ fm $\gg r$ = 2.84 fm, $k = E_\gamma/(\hbar c)$, $kr = E_\gamma r/(\hbar c) \approx 4.3 \times 10^{-3}$ at 300 keV and $\sigma_0 = \pi\, r^2 \approx 2.5 \times 10^{-25}$ cm^2; $m = 2$ corresponds to dipole-like behavior, m = 4 quadrupole like, and m = 6 higher multipole-like. Figure 6 shows that considerably small photodissociation cross sections are possible because SH is much smaller than the photon wavelengths in this thermal energy range.

https://doi.org/10.3390/physics8030064

The significance of this illustrative estimate is as follows. For ordinary atomic photo-absorption, E1 (electric dipole) usually dominates. However, SH is not an ordinary atom. SH is electrically neutral, quite compact, and if nearly spherically symmetric, then the dipole matrix element can be strongly suppressed. If the dipole term vanishes by symmetry, then m = 4 or even m = 6 may become the leading contribution; that will radically improve SH survival.

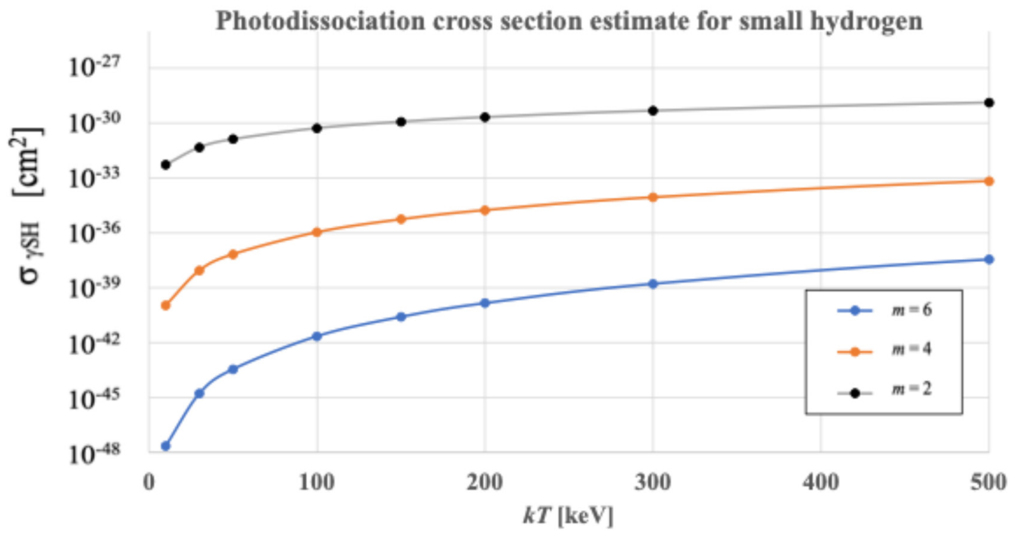

Figure A1. Photodissociation cross sections $\sigma_{\gamma \mathrm{SH}} \propto \sigma_0\ (kr)^m$ as a function of thermal energy for dipole-like (m = 2), quadrupole-like (m = 4) and higher multipole-like (m = 6) behaviour calculated for SH radius r = 2.84 fm, SH binding energy E_b = −308 keV and $\sigma_0 = \pi\, r^2 \approx 2.5 \times 10^{-25}$ cm^2. See text for details.

Appendix E. Maximum SH Destruction Cross Section $\sigma_{\mathbf{dest}}^{\mathbf{max}}$

The quantity $n_\gamma\ (E_\gamma > |E_\mathrm{b}|)$ denotes the number density of photons with energies exceeding the photodissociation threshold $|E_\mathrm{b}|$ and is given by [6,7]

$$n_\gamma(E_\gamma\ > |E_\mathrm{b}|) = \frac{1}{\pi^2}\left(\frac{kT}{\hbar c}\right)^3 \int_x^\infty \frac{u^2 du}{.e^u - 1}. \quad \text{(A1)}$$

Dividing Equation (A1) by the total photon density $n_\gamma = (2\,\zeta(3)/\pi^2)(kT/\hbar c)^3$, where $n_\gamma \equiv\ n_\gamma^{\mathrm{total}}$ is calculated in Appendix A, one obtains:

$$\frac{n_\gamma(E >\ E_\mathrm{b})}{n_\gamma^{\mathrm{total}}} = \frac{1}{2\zeta(3)}\int_x^\infty \frac{u^2 du}{e^u - 1} \approx \frac{x^2 + 2x + 2}{2\zeta(3)}\, e^{-x}, \quad \text{(A2)}$$

where $2\zeta(3) \approx 2.404$ and $x = |E_\mathrm{b}|/kT$; the approximation in Equation (A2) is valid for $x \geq 2$, or for $kT \leq 150$ keV for E_b = 308 keV. That is where SH survival is most relevant. For smaller values of x, the exact integral of Equation (A1) is used when generating the numerical results.

More generally, the photodissociation probability is

$$P_{\mathrm{dest}} = \int_{t_\mathrm{i}}^{t_\mathrm{f}} \Gamma_{\mathrm{dest}} dt = \int_{t_\mathrm{i}}^{t_\mathrm{f}} n_\gamma(E_\gamma > |E_\mathrm{b}|, t)\ \sigma_{\gamma \mathrm{SH}} c\ dt.$$

If the photodissociation cross section varies only weakly over the temperature interval of interest, the photodissociation rate is $\Gamma_{\mathrm{dest}} = [n_\gamma(E_\gamma > |E_\mathrm{b}|)\ \sigma_{\gamma \mathrm{SH}}\ c]$ in units s^{-1}, and the probability may be approximated by $P_{\mathrm{dest}} \approx \Gamma_{\mathrm{dest}} t(kT)$. Requiring $P_{\mathrm{dest}} \leq 1$, equivalently

$\Gamma_{\text{dest}}\, t(kT) \leq 1$, and solving for the largest photodissociation cross section compatible with survival gives

$$\sigma_{\text{dest}}^{\max} = \frac{1}{n_\gamma(E_\gamma > |E_{\text{b}}|)c\, t(kT)} \approx \frac{1}{n_\gamma^{\text{total}} \frac{(2+2x+x^2)}{2\zeta(3)} e^{-x}\, c\, t(kT)}. \quad \text{(A3)}$$

Appendix F. Open Questions

The following open questions remain.

Microscopic Physics

- Calculate SH formation and photodissociation cross sections.
- Calculate SH–nucleus interaction cross sections.
- Determine whether electric dipole (E1) transitions are suppressed.

Cosmology

- Determine BBN constraints on f_{SH}.
- Determine CMB constraints on hidden baryonic SH.
- Calculate SH decoupling temperature more rigorously.
- A more realistic treatment would solve the kinetic abundance equation

$$\frac{dn_{\text{SH}}}{dt} = n_{\text{p}} n_{\text{e}} \langle \sigma v \rangle_{\text{form}} - n_{\text{SH}} \Gamma_{\text{dest}}$$

  rather than using the phenomenological constraints derived in the present paper. Such calculations permit a self-consistent evolution of the SH abundance in the expanding Universe and allow comparison with BBN and CMB observations.

Structure Formation

- Calculate growth of SH density perturbations $\delta_{\text{SH}}(t)$.
- Determine whether SH behaves similarly to a cold dark matter component.
- Investigate possible formation of early black holes [15–18].

Observational Tests

- At present, neither the SH formation cross section nor the SH photodissociation cross section is known theoretically or experimentally. Direct laboratory measurements are expected to be challenging because the pair densities characteristic of the early Universe cannot be reproduced in present-day experiments. If SH exists, possible observational tests include searches for the predicted gamma-ray signature and dedicated analyses of existing high-energy collision data for anomalous electron–proton resonances discussed in Ref. [1]. Such observations could provide independent constraints on the SH hypothesis.

References

1. Va'vra, J. A simple argument that small hydrogen may exist. *Physics* **2026**, *8*, 45. [CrossRef]
2. Kaplan, D.E.; Krnjaic, G.Z.; Rehermann, K.R.; Wells, C.M. Atomic dark matter. *J. Cosmol. Astropart. Phys.* **2010**, *05*, 021. [CrossRef]
3. Cyr-Racine, F.; Sigurdson, K. Cosmology of atomic dark matter. *Phys. Rev. D* **2013**, *87*, 103515. [CrossRef]
4. Cline, J.M. Dark atoms and composite dark matter. *SciPost Phys. Lect. Notes* **2022**, *2021-07: Dark Matter*, 52. [CrossRef]
5. Wagoner, R.V. Big-Bang nucleosynthesis revisited. *Astrophys. J.* **1973**, *179*, 343–360. [CrossRef] [PubMed]
6. Natarajan, P.; Pacucci, F.; Ricarte, A.; Bogdán, Á.; Goulding, A.D.; Cappelluti, N. First detection of an overmassive black hole galaxy UHZ1: Evidence for heavy black hole seed formation from direct collapse. *Astrophys. J. Lett.* **2024**, *960*, L1. [CrossRef]

7. Juodžbalis, I.; Maiolino, R.; Baker, W.M.; Tacchella, S.; Scholtz, J.; D'Eugenio, F.; Witstok, J.; Schneider, R.; Trinca, A.; Valiante, R.; et al. A dormant, over-massive black hole in the early Universe. *Nature* **2024**, *636*, 594–597. [CrossRef] [PubMed]
8. Prole, L.R.; Regan, J.A.; Mehta, D.; Coles, P.; Dayal, P. Primordial black holes in cosmological simulations: Growth prospects for supermassive black holes. *Open J. Astrophys.* **2025**, *8*, 143643. [CrossRef]
9. Weinberg, S. *Cosmology*; Oxford University Press: Oxford, UK, 2008. [CrossRef]
10. Kolb, E.W.; Turner, M.S. *The Early Universe*; Addison-Wesley Publishing Company: Reading, MA, USA, 1990. Available online: https://archive.org/details/earlyuniverse0000kolb (accessed on 8 August 2026).
11. Dodelson, S. *Modern Cosmology*; Academic Press: San Diego, CA, USA, 2003. [CrossRef]
12. Olive, K.A.; Schramm, D.N.; Steigman, G.; Walker, T.P.; Kang, H.S. Big-bang nucleosynthesis revisited. *Phys. Lett. B* **1990**, *236*, 454–460. [CrossRef]
13. Cyburt, R.H.; Fields, B.D.; Olive, K.A.; Yeh, T.-H. Big bang nucleosynthesis: Present status. *Rev. Mod. Phys.* **2016**, *88*, 015004. [CrossRef]
14. Pitrou, C.; Coc, A.; Uzan, J.-P.; Vangioni, E. A new tension in the cosmological model from primordial deuterium? *Mon. Not. R. Astron. Soc. (MNRAS)* **2021**, *502*, 2474–2481. [CrossRef]
15. Smirnov, J. Dark matter bound states: A window into the early universe. *SciPost Phys. Proc.* **2023**, *12*, 003. [CrossRef]
16. Petraki, K.; Socha, A.; Vasilaki, C. The role of unitarization on dark-matter freeze-out via metastable bound states. *J. Cosmol. Astropart. Phys.* **2025**, *2025*, 026. [CrossRef]
17. Prole, L.R.; Regan, J.A.; Mehta, D.; Pakmor, R.; Koudmani, S.; Bourne, M.A.; Glover, S.C.O.; Wise, J.H.; Klessen, R.S.; Tremmel, M.; et al. Black hole feedback, galaxy quenching and outflows at cosmic dawn: Analysis of the SEEDZ simulations. *Open J. Astrophys.* **2026**, *9*, 163549. [CrossRef]
18. Mehta, D.H.; Regan, J.A.; Prole, L. Growth of light seed black holes in the early Universe. *Nat. Astron* **2026**, *10*, 583–592. [CrossRef]

https://doi.org/10.3390/physics8030064